

## Article

# A Synthetic Analog of the Mineral Ivanyukite: Sorption Behavior to Lead Cations

Gleb O. Samburov <sup>1,\*</sup>, Galina O. Kalashnikova <sup>2</sup>, Taras L. Panikorovskii <sup>1</sup>, Vladimir N. Bocharov <sup>3</sup>, Aleksandr Kasikov <sup>4</sup>, Ekaterina Selivanova <sup>2,5</sup>, Ayya V. Bazai <sup>2,5</sup>, Daria Bernadskaya <sup>6</sup>, Viktor N. Yakovenchuk <sup>2,4</sup> and Sergey V. Krivovichev <sup>2</sup>

- <sup>1</sup> Laboratory of Nature-Inspired Technologies and Environmental Safety of the Arctic, Kola Science Centre, Russian Academy of Sciences, 184209 Apatity, Russia; t.panikorovskii@ksc.ru
- <sup>2</sup> Nanomaterials Research Centre, Kola Science Centre, Russian Academy of Sciences, 184209 Apatity, Russia; g.kalashnikova@ksc.ru (G.O.K.); selivanova@geoksc.apatity.ru (E.S.); bazai@geoksc.apatity.ru (A.V.B.); yakovenchuk@geoksc.apatity.ru (V.N.Y.); s.krivovichev@ksc.ru (S.V.K.)
- <sup>3</sup> Geo Environmental Centre “Geomodel”, Saint-Petersburg State University, 198504 St. Petersburg, Russia; bocharov@molsp.phys.spbu.ru
- <sup>4</sup> I.V. Tananaev Institute of Chemistry and Technology of Rare Elements and Mineral Raw Materials, Kola Science Centre, Russian Academy of Sciences, 184209 Apatity, Russia; a.kasikov@ksc.ru
- <sup>5</sup> Geological Institute, Kola Science Centre, Russian Academy of Sciences, 184209 Apatity, Russia
- <sup>6</sup> Institute of the North Industrial Ecology Problems, Kola Science Centre, 184209 Apatity, Russia; d.bernadskaya@ksc.ru
- \* Correspondence: g.samburov@ksc.ru; Tel.: +7-921-030-88-75



**Citation:** Samburov, G.O.; Kalashnikova, G.O.; Panikorovskii, T.L.; Bocharov, V.N.; Kasikov, A.; Selivanova, E.; Bazai, A.V.; Bernadskaya, D.; Yakovenchuk, V.N.; Krivovichev, S.V. A Synthetic Analog of the Mineral Ivanyukite: Sorption Behavior to Lead Cations. *Crystals* **2022**, *12*, 311. <https://doi.org/10.3390/cryst12030311>

Academic Editor: Francesco Capitelli

Received: 31 January 2022

Accepted: 21 February 2022

Published: 23 February 2022

**Publisher’s Note:** MDPI stays neutral with regard to jurisdictional claims in published maps and institutional affiliations.



**Copyright:** © 2022 by the authors. Licensee MDPI, Basel, Switzerland. This article is an open access article distributed under the terms and conditions of the Creative Commons Attribution (CC BY) license (<https://creativecommons.org/licenses/by/4.0/>).

**Abstract:** The production of electrolytic nickel includes the stage of leaching of captured firing nickel matte dust. The solutions formed during this process contain considerable amounts of Pb, which is difficult to extraction due to its low concentration upon the high-salt background. The sorption of lead from model solutions with various compositions by synthetic and natural titanosilicate sorbents (synthetic ivanyukite-Na-T (SIV), ivanyukite-Na-T, and AM-4) have been investigated. The maximal sorption capacity of Pb is up to 400 mg/g and was demonstrated by synthetic ivanyukite In solutions with the high content of Cl<sup>−</sup> (20 g/L), extraction was observed only with a high amount of Na (150 g/L). Molecular mechanisms and kinetics of lead incorporation into ivanyukite were studied by the combination of single-crystal and powder X-ray diffraction, microprobe analysis, and Raman spectroscopy. Incorporation of lead into natural ivanyukite-Na-T with the *R*3m symmetry by the substitution 2Na<sup>+</sup> + 2O<sup>2−</sup> ↔ Pb<sup>2+</sup> + □ + 2OH<sup>−</sup> leads to its transformation into the cubic *P*–43m Pb-exchanged form with the empirical formulae Pb<sub>1.26</sub>[Ti<sub>4</sub>O<sub>2.52</sub>(OH)<sub>1.48</sub>(SiO<sub>4</sub>)<sub>3</sub>]·3.32(H<sub>2</sub>O).

**Keywords:** ivanyukite; lintisite; SIV; AM-4; synthesis; sorption; lead; ion-exchange; titanosilicate; Arctic

## 1. Introduction

Minerals of the ivanyukite group were discovered in 2009 by Yakovenchuk and co-authors in a pegmatite vein of the Koashva apatite mine, Khibiny Massif, Kola Peninsula, Russia [1]. Ivanyukite group minerals have been found in several varieties including ivanyukite-Na-T (*T*—rhombohedral form), ivanyukite-Na-C (*C*—cubic form), ivanyukite—K, and ivanyukite—Cu. The observed chemical diversity was assigned to the high ion-exchange and sorption capacities of the minerals.

In contrast to othertitanosilicates discovered in the Khibiny Massif or Lovozero Massif (Kola Peninsula, Russia)—such as lintisite, zorite and sitinakite [2–7]—the synthetic of ivanyukite was known prior to its mineralogical discovery, being obtained by D. Chapman and A. Roe in 1990 [8] under the name ‘grace titanium silicate’ (GTS). For their synthesis process, the authors had used Ti(OC<sub>2</sub>H<sub>5</sub>)<sub>4</sub> as a source of Ti. The synthetic titanosilicate AM-4 was first obtained by M.S. Dadachov in 1997 using TiCl<sub>3</sub> as a starting reagent [9].

In this work, the synthesis of ivanyukite and AM-4 was done using different Ti sources. For example, semi-product ( $\text{TiCl}_4$ ) of hydrochloric acid loparite ore treatment (JSC “Solikamsk Magnesium Works”, Solikamsk, Russia) [10] and a semi-product (ammonium titanysulfate  $(\text{NH}_4)_2\text{TiO}(\text{SO}_4)_2 \cdot \text{H}_2\text{O}$ ) of sulfuric acid titanite ore treatment (mining JSC “Apatit”, PhosAgro, Russia) [11,12] were used extensively, providing a link between industrially available compounds and a new material with potential innovative applications.

There are human health risks associated with the lead exposure and are important for industrial areas and surrounding cities. For example, in the Monchegorsk city area (Kola peninsula) the nickel and copper pollution is by 6–1500 times higher than the European background levels [13]. Analysis of trace metals by atomic adsorption spectroscopy [14] showed that the highly Pb-polluted waters of the Kola Peninsula reached 425-times the background concentration ( $8 \mu\text{g/L}$ ) in areas of anthropogenic impact compared to the background level of the Murmansk region [14]. The concentration of Pb is more than 19-times higher than the reference recommended values of maximum tolerable concentrations of this element in soils around copper–nickel metallurgical smelters [15–17].

Since this work was carried out taking into account the principle of integrated nature management, one of the subjects of research was both models and real samples of solutions of the nickel–copper plant JSC “Severonickel KMM” (Monchegorsk, Russia). These solutions are characterized by a low concentrations of Ag and Pb cations ( $0.3 \text{ g/L}$  and up to  $1 \text{ g/L}$ , respectively) with the high concentrations of NaCl or  $\text{NaSO}_4$  (up to  $200 \text{ g/L}$ ).

For the purification of silver-containing solutions, a new technique has been developed and a patent application RU 2021124566A has been filed [16]. In this work, we propose new conditions (molar ratio, temperature, and volume) for the synthesis of the AM-4 and SIV titanosilicates and test their sorption properties with respect to Pb for different solutions. The molecular mechanism and kinetics of Pb incorporation into ivanyukite structure has been studied here in detail.

## 2. Materials and Methods

### 2.1. Materials and Their Abbreviations

SIV—is a synthetic titanosilicate material with the composition  $\text{Na}_4(\text{TiO})_4(\text{SiO}_4)_3 \cdot n\text{H}_2\text{O}$  that possesses a microporous crystal structure similar to that observed in ivanyukite-group minerals [1].

AM-4—is a synthetic analog of the mineral lintsite that is used in this work for comparison of its sorption properties with those of SIV was obtained according to the methodology described in detail in [3,18,19].

SL3—is the protonated form of AM-4 obtained according to the methods described in [3,18].

STA—is ammonium sulfate oxytitanium,  $(\text{NH}_4)_2\text{TiO}(\text{SO}_4)_2 \cdot \text{H}_2\text{O}$ , the pre-product of titanite concentrate reprocessing (PJSC “PhosAgro”, Apatity, Russia) [20].

### 2.2. Reagents

Titanium tetrachloride (JSC “Solikamsk Magnesium Works”, Solikamsk, Russia) and  $(\text{NH}_4)_2\text{TiO}(\text{SO}_4)_2 \cdot \text{H}_2\text{O}$  (PJSC PhosAgro, Apatity, Russia) were of technical grade quality; sodium hydroxide (Aldrich, Moscow, Russia) was of ACS grade quality; sodium metasilicate, lead nitrate, and sodium chloride produced by the Neva Reactive were of U.S.P. grade quality. The solutions 1–7 were model and real solutions after processing (leaching) of fine dusts of nickel production generated by the pyrometallurgical processes at metallurgical plants and captured by electrostatic precipitators during dry cleaning of dust and gas phases.

### 2.3. Synthesis

Sodium metasilicate and titanium tetrachloride (or ammonium sulfate oxytitanium) were taken according to their molar ratios of  $\text{Na}_2\text{O}:\text{SiO}_2:\text{TiO}_2:\text{H}_2\text{O} = 4.5:4:1:160$  [9,16] and  $5.6:3.1:1:128$ , for the synthesis of SIV and of AM-4, respectively. The mixture of initial reagents was dissolved in a distilled water at 298 K and stirred with the mixing speed of

200 revolutions per minute during 4 h to obtain SIV powders. The autoclaves with the mixtures were maintained under hydrothermal conditions (453 K, 1.5 MPa) for 96 h (in the case of  $\text{TiCl}_4$ ) and 48 h (in the case of ammonium sulfate oxytitanium). The product were filtered by vacuum flask, washed by distilled water (1/5 of the total mixture volume), and dried at 348 K.

Autoclaves with the volumes of 40 cm<sup>3</sup> and 450 cm<sup>3</sup> (production of FRC Kola Science Centre, Apatity, Russia) were used for the hydrothermal synthesis of the SIV. The autoclave with volume of 7 L (Parr Instrument Company, Moline, IL, USA) was used for SIV synthesis only. The SIV powders were firstly obtained with the initial molar ratio of  $\text{Na}_2\text{O}:\text{SiO}_2:\text{TiO}_2:\text{H}_2\text{O} = 5.6:3.1:1:128$  under 373 K.

The high precision universal drying oven SNOL (SNOL-TERM, Utena, Lithuania), with the operating temperature range from 323 to 573 K and programmable thermostat, was used for heating autoclaves and for power drying.

The synthesized powders were separated from the mother liquor by vacuum filtration using a diaphragm pump (Technology for Vacuum system, Vacuubrand, Wertheim, Germany).

In all cases where mixing was necessary, a magnetic stirrer IKA RT 5 (Germany) was used.

The drying process of the powder was carried out for 4 h at 348 K using the SNOL drying oven (SNOL-TERM, Utena, Lithuania).

Sartorius—ED224S-RCE (Sartorius, Goettingen, Germany) was the first class accuracy analytical balance used for weighing synthetic titanosilicate powders and reagents.

#### 2.4. Composition

Investigation of morphology of the Pb-exchanged ivanyukite samples was carried out using a scanning electron microscope LEO-1450 (Carl Zeiss Microscopy, Oberkochen, Germany) and chemical composition was studied with an Oxford Instruments Ultim Max 100 analyzer at 20 kV, 500–1000 pA, 1–3  $\mu\text{m}$  beam diameter (Geological Institute of Kola Science Centre, Apatity, Russia).

The content of Pb in the samples was determined by the inductively coupled plasma atomic emission spectrometry (ICP AES, Institute of the North Industrial Ecology Problems of Kola Science Centre, Apatity, Russia). To construct the calibration curve, a multi-element standard sample of  $\text{Pb}^{2+}$  ions GSO 7877-2000 was used. The samples were diluted with 2% nitric acid in a ratio of 1:100. The 2% nitric acid was obtained by mixing purified water—18.2  $\text{M}\Omega \times \text{cm}$  (Ultra Clear TP UV UF TM, EVOQUA, Pittsburgh, PA, USA) with distilled nitric acid obtained by an acid distillation unit (SPK-2, Saint-Petersburg, Russia).

The obtained solutions were analyzed by an “Optima 2100 DV” (PerkinElmer, Waltham, MA, USA) an inductively coupled plasma atomic emission spectrometer with the following settings: wavelength 220.353 nm; axial torch viewing position; nebulizer gas flow 0.8 L/min; flow rate 1.5 mL/min; power 1300 Watts (Institute of the North Industrial Ecology Problems of Kola Science Centre, Apatity, Russia). The method of standard addition was used to estimate the validity of the analysis.

#### 2.5. Pb Sorption from the Simulated Model Solution

The possibility of extracting Pb from its solutions by employing titanosilicates was studied using nitrate salt. For this purpose, the  $\text{Pb}(\text{NO}_3)_2$  solutions containing 0.39, 0.88, and 1.79 g/L of Pb (initial solutions 1–3) were prepared by dissolving in 1000 cm<sup>3</sup> of distilled water 0.62, 1.4, and 2.87 g of  $\text{Pb}(\text{NO}_3)_2$  respectively. The sorption experiments were conducted by the immersion of titanosilicate powders into solutions at 298 K for 4 h with a constant stirring. The ratio of liquid and solid phases was  $V:m = 50:0.5$  (mL:g) in each experiment. After sorption, the powders were filtered by vacuum filtration, washed with distilled water in three steps (50 mL for each step), and dried at 348 K. For each experiment, a parallel control experiment was conducted.

### 2.6. Pb Sorption from the Dust Leaching Solution (Model Solution)

Before starting work with a real solution of leaching of nickel Feinstein firing dusts, an experiment was conducted on a model solution, simulating the composition of industrial solutions. In order to prepare the latter, 60 mL of NaCl solution with the concentration 333 g/L (20 g NaCl dissolved in 60 mL of distilled water) and 20 mL of Pb(NO<sub>3</sub>)<sub>2</sub> solution with a concentration 6.5 g/L (0.13 g Pb(NO<sub>3</sub>)<sub>2</sub> dissolved in 20 mL of distilled water) were added with a small portion of 20 mL AgNO<sub>3</sub> solution at a concentration of 0.8 g/L (0.016 g AgNO<sub>3</sub> dissolved in 20 mL of distilled water); the resulting solution was diluted in 400 mL of Na<sub>2</sub>SO<sub>4</sub> solution with a concentration of 95 g/L. The experimental conditions agreed well with the conditions described for the experiments with a model solution Pb(NO<sub>3</sub>)<sub>2</sub> with a difference in a liquid–solid ratio, which in this case was equal to V:m = 25:0.25 (cm<sup>3</sup>:g). The SL3 sorbent was not used in the experiments with the first model solutions because of its low efficiency in recent studies. For each experiment, a parallel control experiment was conducted.

### 2.7. Pb Sorption from the Dust Leaching Solution (Real Solution)

Two different solutions of leaching of fine dusts of nickel production firing dusts from copper-nickel plant JSC “Severonickel KMM” were used in this study as provided by the industrial plant laboratory. The first one, solution-6, was obtained by the treatment the fine-grained dust of nickel production with a solution of sodium chloride with the concentration of 200 g/L and precipitation of Pb with a solution of sodium sulphate with the concentration 200 g/L. The second one, solution-7, was a product of the dusts of nickel production treatment similar to solution-6, except for that leaching was carried out with a solution of sulfuric acid with the concentration of 200 g/L. The conditions of the sorption experiments were same as those implemented for model solutions.

For each experiment, a second parallel experiment was conducted for control purposes.

The cation-exchange capacity of the sorbent (mg/g) in each experiment was calculated by Equation (1)

$$q = (C_0 - C_e) \cdot (V/m) \quad (1)$$

where C<sub>0</sub>—is the initial concentration of the element in the solution (mg/L); C<sub>e</sub>—is the equilibrium concentration of the element in the solution after sorption (mg/L); V—is the volume of solution (L); m—is the mass of the sorbent (g).

The extent of extraction of the element (%) was calculated by Equation (2)

$$A = \frac{C_0 - C_e}{C_0} \cdot 100 \quad (2)$$

where C<sub>0</sub>—the initial concentration of the element in the solution (mg/L); C<sub>e</sub>—the equilibrium concentration of the element in the solution after sorption (mg/L).

### 2.8. Raman Spectroscopy

The Raman spectra (RS) of SIV, SIV-Pb, and Pb-exchanged form of ivanyukite collected from uncoated individual grains were recorded with a Horiba Jobin-Yvon LabRAM HR800 spectrometer (Horiba, Kyoto, Japan) equipped with an Olympus BX-41 microscope (Olympus Corporation, Tokyo, Japan) in backscattering geometry (Saint-Petersburg State University, Saint-Petersburg, Russia). Raman spectra were excited by a solid-state laser (532 nm) with an actual power of 2 mW under the 50× objective (NA 0.75). The spectra were obtained in a range of 70–4000 cm<sup>−1</sup> at a resolution of 2 cm<sup>−1</sup> at room temperature. To improve the signal-to-noise ratio, the number of acquisitions was set to 15. The spectra were processed using the algorithms implemented in Labspec (Horiba, Kyoto, Japan) and OriginPro 8.1 (OriginLab Corporation, Northampton, MA, USA) software packages.

### 2.9. Powder and Single-Crystal X-ray Diffraction

The synthetic products were investigated by means of powder X-ray diffraction using a Bruker D2 Phaser diffractometer (Bruker Corporation, Billerica, MA, USA) (CuK $\alpha$  radiation, 30 kV/10 mA) (XRD Research Center, St. Petersburg State University, Saint-Petersburg, Russia). The experiments were carried out in the  $2\theta$  range 5–65 ( $^\circ$ ) with a step of 0.02 $^\circ$ , and the exposure at each point was 1 s.

The crystal-structure study of Pb-exchanged ivanyukite was carried out at the X-ray Diffraction Resource Centre of St. Petersburg State University (Saint-Petersburg, Russia) by means of the Synergy S single-crystal diffractometer equipped with a Hypix (Rigaku Corporation, Tokyo, Japan) detector using monochromatic MoK $\alpha$  radiation ( $\lambda = 0.71069 \text{ \AA}$ ) at room temperature. More than a half of the diffraction sphere was collected with scanning step of 1 $^\circ$ , and an exposure time of 30 s. The data were integrated and corrected by means of the CrysAlis (Rigaku Corporation, Tokyo, Japan) program package, which was also used to apply empirical absorption correction using spherical harmonics, implemented in the SCALE3 ABSPACK scaling algorithm [21]. The structure was refined using the SHELXL software package [21]. The crystal structure was drawn using the VESTA 3 program [22]. Occupancies of the cation sites were calculated from the experimental site-scattering factors (except for the low-occupied sites) in accordance with the empirical chemical composition. Hydrogen sites could not be located.

The SCXRD data are deposited in CCDC under entry no. 2130913. Crystal data, data collection information, and refinement details are given in Table 1. Atom coordinates and isotropic parameters of atomic displacements are given in Table S1, interatomic distances in Table S2, and the anisotropic parameters of atomic displacements are given in Table S3.

**Table 1.** Crystal data, data collection information, and refinement details Pb-exchanged form ivanyukite.

| Temperature/K                                  | 293 (2)  |
|--|--|
| Crystal system                                 | cubic  |
| Space group                                    | <i>P</i> -43m  |
| $a = b = c/\text{\AA}$                         | 7.8037 (7)   |
| $\alpha = \beta = \gamma/^\circ$               | 90   |
| Volume/ $\text{\AA}^3$                         | 475.23 (13)  |
| <i>Z</i>                                       | 1  |
| $\rho_{\text{calc}}/\text{g/cm}^3$             | 2.956  |
| $\mu/\text{mm}^{-1}$                           | 13.003   |
| <i>F</i> (000)                                 | 388.0  |
| Crystal size/ $\text{mm}^3$                    | $0.12 \times 0.12 \times 0.12$                               |
| Radiation                                      | Mo K $\alpha$ ( $\lambda = 0.71073$ )                        |
| $2\theta$ range for data collection/ $^\circ$  | 7.384 to 52.998  |
| Index ranges                                   | $-6 \leq h \leq 9, -9 \leq k \leq 4, -9 \leq l \leq 9$       |
| Reflections collected                          | 612  |
| Independent reflections                        | 200 [ $R_{\text{int}} = 0.0486, R_{\text{sigma}} = 0.0310$ ] |
| Data/restraints/parameters                     | 200/0/23   |
| Goodness-of-fit on $F^2$                       | 1.116  |
| Final <i>R</i> indexes [ $I \geq 2\sigma(I)$ ] | $R_1 = 0.0497, wR_2 = 0.1186$                                |
| Final <i>R</i> indexes [all data]              | $R_1 = 0.0644, wR_2 = 0.1257$                                |
| Largest diff. peak/hole/ $e \text{ \AA}^{-3}$  | 0.71/−0.64   |
| Flack parameter                                | 0.008(19)  |

## 3. Results

### 3.1. Composition

Natural ivanyukite contains numerous intergrowths of aegirine (Figure 1a). Pb-exchanged natural ivanyukite contains up to 0.04 apfu of Fe $^{2+}$  and 0.12 apfu of Nb $^{5+}$ , whereas its synthetic counterpart may contain up to 0.09 apfu of Al $^{3+}$ . The SIV aggregates are represented by a fine-grained matrix with nanometer-sized crystallites (Figure 1b). AM-

4 forms rosette-like aggregates with the size of individual crystals less than  $100 \times 100 \times 10 \mu\text{m}$  (Figure 1f). Both samples of Pb-exchanged SIV and AM-4 (Figure 1c,e) contained an admixture of prismatic crystals of  $\text{Pb}_3\text{O}_4$  (Figure 1d).

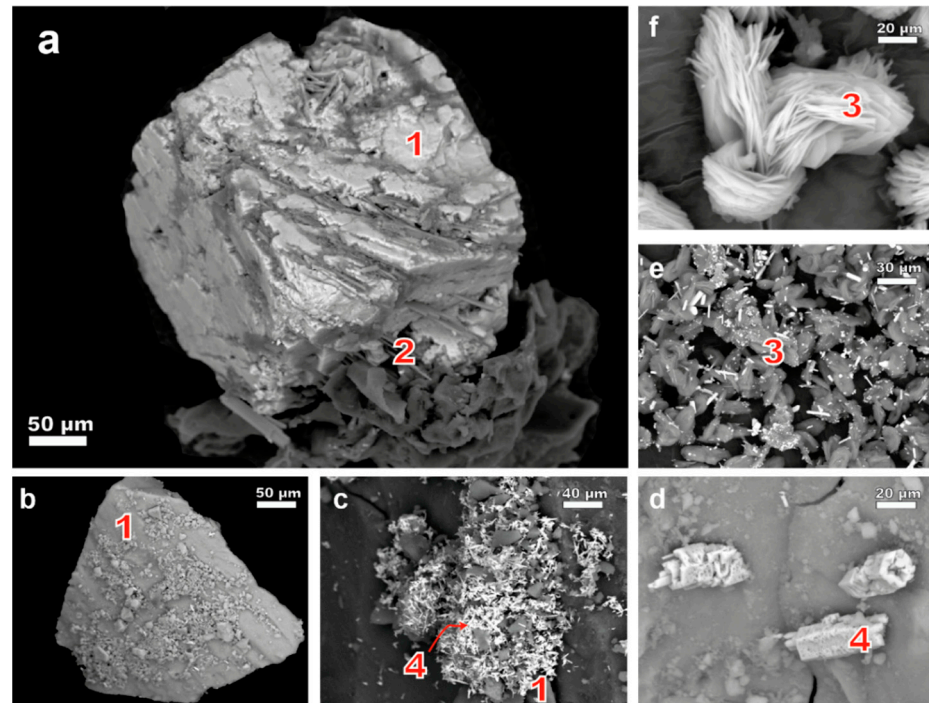


**Figure 1.** Backscattered images of (a) Pb-exchanged natural ivanyukite (1) with aegirine (2) inclusion; (b) Pb-exchanged SIV; (c) formation of  $\text{Pb}_3\text{O}_4$  (4) crystals on the surface of Pb-exchanged SIV; (d) individual prismatic crystals of  $\text{Pb}_3\text{O}_4$ ; (e) Pb-exchanged AM-4 (3); (f) AM-4 rosette-like aggregates.

The Pb-exchanged SIV contains residual 0.06–0.36 apfu of  $\text{K}^+$ . Both synthetic and natural ivanyukite demonstrate exceptional ion-exchange properties close to the ideal substitution scheme  $2\text{Na}^+ \leftrightarrow 1\text{Pb}^{2+} + 1\text{□}$ . Table 2 provides analytical results for natural and synthetic ivanyukite and their Pb-exchanged forms.

**Table 2.** Chemical composition of Pb-exchanged SIV and Pb-exchanged natural ivanyukite.

| Constituent             | Pb-Exchanged SIV |       |        | Pb-Exchanged Natural Ivanyukite |       |
|-------------------------|------------------|-------|--------|---------------------------------|-------|
| $\text{SiO}_2$          | 18.11            | 19.08 | 19.40  | 18.23                           | 19.23 |
| $\text{TiO}_2$          | 30.74            | 30.01 | 31.64  | 31.65                           | 32.50 |
| $\text{Al}_2\text{O}_3$ | 0.45             |       | 0.23   |                                 |       |
| FeO                     |                  |       |        | 0.22                            | 0.31  |
| $\text{Nb}_2\text{O}_5$ |                  |       |        | 1.64                            | 1.68  |
| $\text{K}_2\text{O}$    | 0.44             | 0.32  | 1.85   |                                 |       |
| PbO                     | 38.60            | 38.40 | 36.03  | 37.59                           | 34.87 |
| $\text{H}_2\text{O}^*$  | 9.70             | 10.00 | 11.00  | 10.10                           | 10.10 |
| Total                   | 98.04            | 97.81 | 100.15 | 99.43                           | 98.69 |
| $\text{Si}^{4+}$        | 3.00             | 3.00  | 3.00   | 3.00                            | 3.00  |
| $\text{Ti}^{4+}$        | 3.83             | 3.55  | 3.68   | 3.92                            | 3.81  |
| $\text{Al}^{3+}$        | 0.09             |       | 0.04   |                                 |       |
| $\text{Fe}^{2+}$        |                  |       |        | 0.03                            | 0.04  |
| $\text{Nb}^{5+}$        |                  |       |        | 0.12                            | 0.12  |
| Sum O                   | 3.92             | 3.55  | 3.72   | 4.07                            | 3.97  |

**Table 2.** *Cont.*

| Constituent      | Pb-Exchanged SIV |       |       | Pb-Exchanged Natural Ivanyukite |       |
|------------------|------------------|-------|-------|---------------------------------|-------|
|                  |                  |       |       |                                 |       |
| K <sup>+</sup>   | 0.09             | 0.06  | 0.36  |                                 |       |
| Pb <sup>2+</sup> | 1.72             | 1.63  | 1.50  | 1.67                            | 1.46  |
| Sum A            | 1.81             | 1.69  | 1.86  | 1.67                            | 1.46  |
| OH <sup>−</sup>  | 10.72            | 10.49 | 11.35 | 11.09                           | 10.51 |

\* The content of H<sub>2</sub>O was calculated according to the ivanyukite formula (4 apfu) and the content of OH according to the charge-balance requirements.

### 3.2. Pb Sorption from the Simulated Model Solution

The concentrations of Pb in the model solutions were determined by atomic emission spectrometry and are given in Table 3.

**Table 3.** Results of sorption experiments of Pb from Pb(NO<sub>3</sub>)<sub>2</sub> solutions.

|                      | C(Pb), g/L | q, mg/g | A, %  |
|----------------------|------------|---------|-------|
| Initial solution 1   | 0.39       |         |       |
| SIV                  | 0.0089     | 38.11   | 97.72 |
| SL3                  | 0.31       | 8       | 20.51 |
| AM-4                 | 0.0008     | 38.92   | 99.79 |
| Initial solution 2   | 0.88       |         |       |
| SIV                  | 0.004      | 87.6    | 99.55 |
| SL3                  | 0.80       | 8       | 9.09  |
| AM-4                 | 0.0009     | 87.91   | 99.90 |
| Initial solution 3   | 1.79       |         |       |
| SIV                  | 0.0026     | 178.74  | 99.85 |
| AM-4                 | 0.0009     | 178.91  | 99.95 |
| Initial solution 4   | 1.78       |         |       |
| SIV                  | 0.97       | 403     | 45.28 |
| AM-4                 | 1.73       | 26      | 2.92  |
| Initial solution 5 * | 0.16       |         |       |
| SIV                  | 0.016      | 14.4    | 90    |
| AM-4                 | 0.017      | 14.3    | 89    |
| Initial solution 6 * | 23.70      |         |       |
| SIV                  | 0.11       | 2.4     | 99.5  |
| AM-4                 | <0.03      | 2.4     | 99.9  |
| Initial solution 7 * | 56.23      |         |       |
| SIV                  | 55.04      | 0.1     | 2.1   |
| AM-4                 | 55.68      | 0.1     | 1.0   |

\* Data on the sorption of silver from solutions are not given due to the registration of the patent RU 2021124566 [17].

The cation-exchange capacity of the sorbents with respect to Pb was up to 178 mg/g for SIV and AM-4 with the extent of extraction of up to 99.85% and 8 mg/g for SL3 in each solution (initial solutions 1–3). In all cases the extent of extraction of Pb by the SIV and AM-4 was more than 99%.

It was found that, under given conditions for Pb sorption from the industrial solutions, both sorbents demonstrated excellent sorption properties with respect to Pb (Table 3, initial solution 5). The cation-exchange capacity for Pb was 14.4 and 14.3 mg/g for SIV and AM-4, respectively, with the extents of extraction equal to 90%.

The extent of Pb extraction from the real dust leaching solution-6 was 99.55% with the cation-exchange capacity for SIV equal to of 13 mg/g. The results of the experiment are presented in Table 3.

### 3.3. Raman Spectroscopy

The Raman spectra of SIV (ivanyukite-Na-T), SIV-Pb, and Pb-exchanged natural ivanyukite are shown in Figure 2. The assignments of the absorption bands were made by analogy with structurally related pharmacosiderite type compounds [23–25] and titanosilicates [26–29].

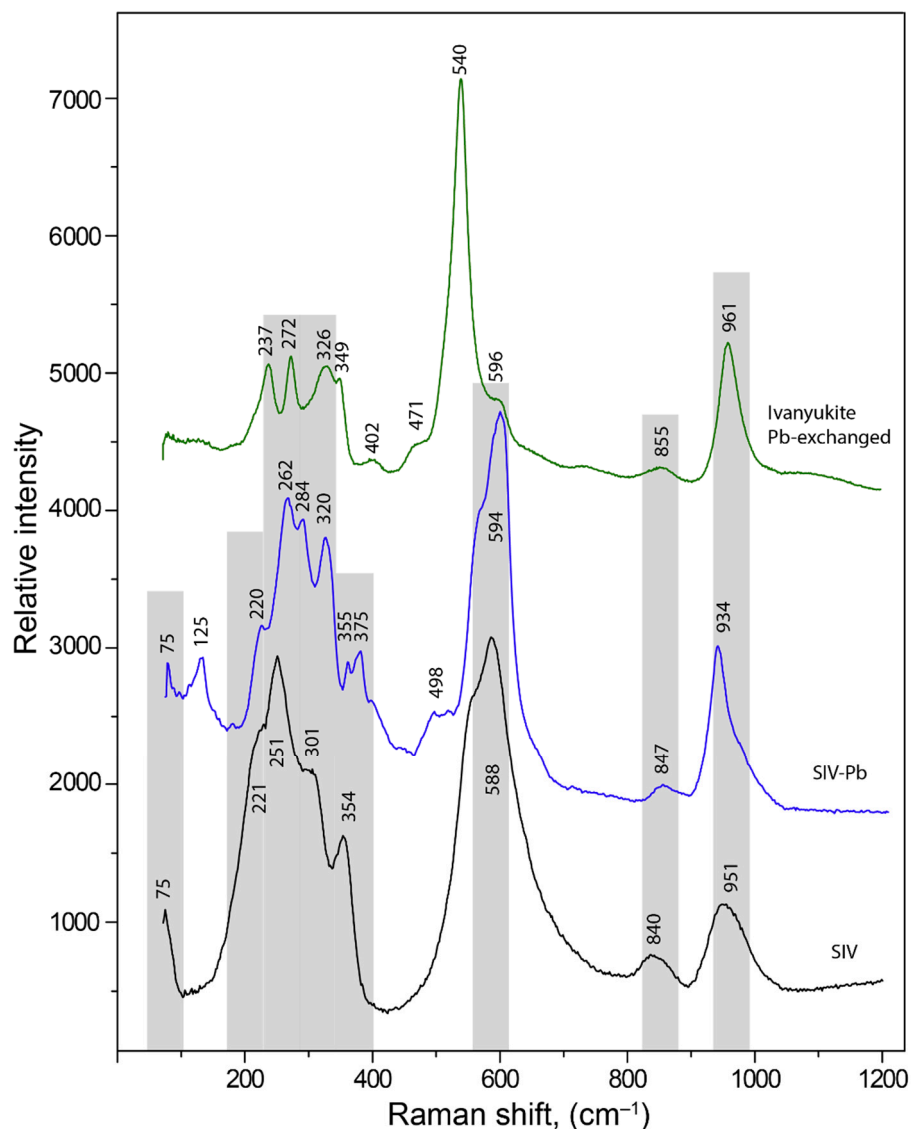


**Figure 2.** Raman spectra of initial SIV, SIV-Pb, and Pb-exchanged natural ivanyukite. The main bands in the initial SIV spectra are indicated by gray lines.

The intense vibrational bands at 951, 934, and 961  $\text{cm}^{-1}$  can be attributed to asymmetric stretching vibrations of  $\text{SiO}_4$  tetrahedra, while the bands at 840, 847, and 855,  $\text{cm}^{-1}$  are assigned to symmetric vibration modes involving the same bonds [24,28]. The most intense bands at 588 and 594  $\text{cm}^{-1}$  for rhombohedral SIV are significantly shifted (by  $\sim 60 \text{ cm}^{-1}$ ) in comparison with the band at 540  $\text{cm}^{-1}$  observed in the spectrum of Pb-exchanged natural ivanyukite and are related to the asymmetric bending vibrations of Si–O bonds or overlapping stretching vibrations of Ti–O bonds [25,28]. The same shift was observed previously for natural ivanyukite and corresponded to the transition from rhombohedral to cubic form [27]. The bands in the range of 350–500  $\text{cm}^{-1}$  correspond to symmetric bending vibrations of O–Si–O bonds and overlapping stretching vibrations of Ti–O bonds [25–27]. The bands at 498 and 471  $\text{cm}^{-1}$  were assigned to different modes of Ti–O stretching

vibrations. Bands of different intensities in the region of  $200\text{--}350\text{ cm}^{-1}$  belong to different bending vibration modes of the Ti–O bonds in  $\text{TiO}_6$  octahedra [23,24]. The bands with the wave numbers below  $200\text{ cm}^{-1}$  belong to translational vibrations. The bands at  $75$  and  $126\text{--}128\text{ cm}^{-1}$  are observed in the Raman spectra of synthetic samples and are absent in the Raman spectrum of the Pb-exchanged natural ivanyukite and probably respond to translation modes of K.

In general, the spectrum of Pb-exchanged natural ivanyukite corresponds to the cubic form, whereas the spectrum of SIV-Pb has characteristic features corresponding to both trigonal and cubic forms. It contains bands near  $498\text{ cm}^{-1}$  that are characteristic of cubic Pb-exchanged natural ivanyukite and at the same time has bands near  $220$  and  $350\text{ cm}^{-1}$  that are characteristic of trigonal SIV. This can be explained by the presence of domains with both trigonal and cubic symmetries within the single grains of SIV-Pb.

### 3.4. Powder Diffraction

The initial XRD pattern of SIV is in good agreement with that of synthetic ivanyukite-Na-T, (PDF Card No. 00-052-1204). Intensity of the (101) reflection significantly decreases after Pb sorption (Figure 3). The appearance of (440) reflection at  $68.18^\circ 2\theta$  ( $1.3743\text{ \AA}$ ) in SIV-Pb instead two peaks at  $67.15$  and  $68.80^\circ 2\theta$  observed in SIV pattern indicates the  $R3m$  to  $P\text{--}43m$  symmetry change. The observed pattern for the Pb-exchanged SIV agrees with that of synthetic ivanyukite-Na-C (PDF Card No.00-047-0042). The increase in the Pb concentration results in the decrease of intensities of main reflections and is probably connected with the increase of absorption coefficient induced by the increases amounts of Pb in the structure. When the maximum sorption capacity is reached, the  $\text{Pb}_3\text{O}_4$  lead oxide (PDF Card No. 01-071-0562) starts to crystallize. The presence of  $\text{Pb}_3\text{O}_4$  was confirmed by our chemical data (Figure 1d) and the presence of additional reflections at  $24.82^\circ 2\theta$  ( $3.584\text{ \AA}$ ),  $25.49^\circ 2\theta$  ( $3.492\text{ \AA}$ ), and  $43.48^\circ 2\theta$  ( $2.079\text{ \AA}$ ).

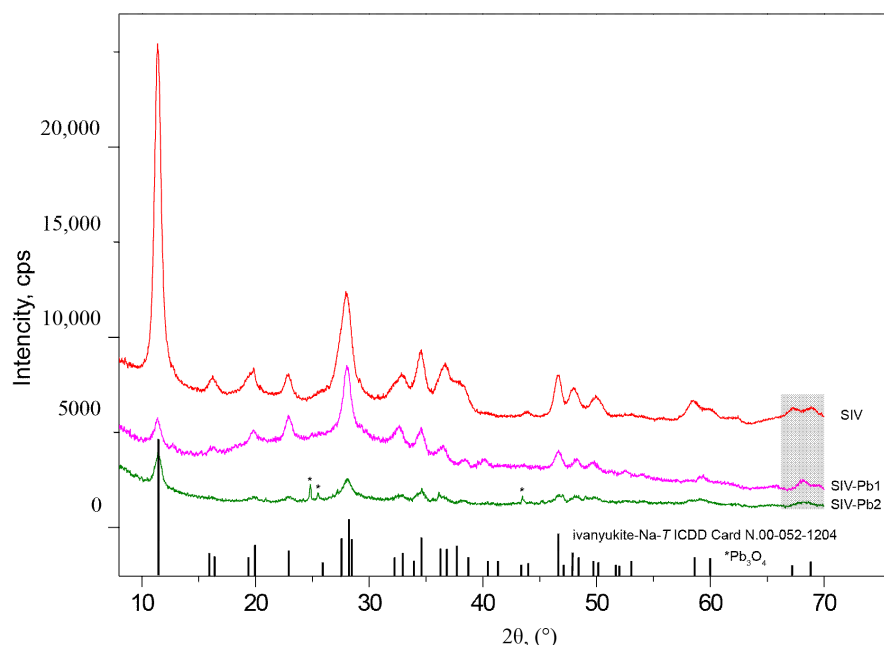


**Figure 3.** Diffraction patterns of SIV (red curve) and its Pb-exchanged forms with the S:L ratios of 1:500 (pink) and 1:133 (green). Asterisks indicate peaks of  $\text{Pb}_3\text{O}_4$ .

### 3.5. Single-Crystal XRD

The crystal structure of Pb-exchanged ivanyukite was refined in the  $P\text{--}43m$  space group to  $R_1 = 0.049$  for 200 ( $R_{int} = 0.049$ ,  $R_{sigma} = 0.030$ ) independent reflections with  $F_o > 4\sigma(F_o)$  using the model of ivanyukite-K [27]. The crystal structure of Pb-exchanged ivanyukite (Figure 4a) possesses a pharmacosiderite structural topology and is based upon

a topologically identical three-dimensional framework [28]. The main structural feature of ivanyukite-group minerals is the presence of cubane-like  $[\text{Ti}_4\text{O}_4]^{8+}$  clusters formed by four edge-sharing  $\text{TiO}_6$  octahedra [29]. The  $[\text{Ti}_4\text{O}_4]^{8+}$  clusters are connected by sharing corners with  $\text{SiO}_4$  tetrahedra to form a negatively charged  $[(\text{TiO})_4(\text{SiO}_4)_3]_4^-$  framework. The framework has a three-dimensional system of channels defined by 8-membered rings (8-MRs) with a free (suitable for migration) crystallographic diameter of  $\sim 3.5$  Å [30]. The channels are occupied by extra-framework cations (e.g.,  $\text{Na}^+$ ,  $\text{K}^+$ ) and  $\text{H}_2\text{O}$  molecules.

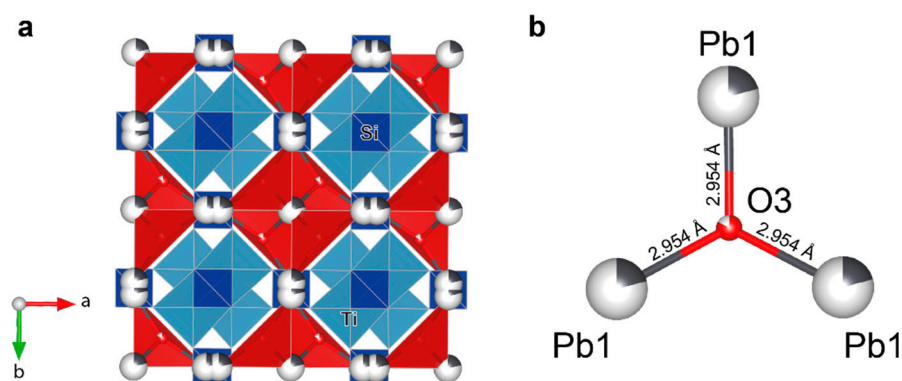


**Figure 4.** Crystal structure of Pb-exchanged ivanyukite in general projection (a); local coordination of Pb in the crystal structure of Pb-exchanged ivanyukite (b).

In the crystal structure of Pb-exchanged ivanyukite, as in other cubicpharmacosiderite-super group minerals [31], there is one symmetrically independent Si1 and one Ti1 site coordinated by the O1 and O2 atoms. The mean bond lengths for  $\text{SiO}_4$  tetrahedra  $\text{TiO}_6$  octahedra are,  $\langle 1.642 \rangle$  Å and  $\langle 1.961 \rangle$  Å, respectively, in good agreement with their full occupancies. The splitted Pb1 site is situated at the center of the 8-MR with the site occupation factor (s.o.f.) = of 0.21 and the Pb–Pb distance of 0.62 Å. The Pb1 site is bonded to two O3( $\text{H}_2\text{O}$ ) sites.

The structural formula of Pb-exchanged ivanyukite determined from the structure refinement can be written as  $\text{Pb}_{1.26}[\text{Ti}_4\text{O}_{2.52}(\text{OH})_{1.48}(\text{SiO}_4)_3] \cdot 3.32(\text{H}_2\text{O})$ .

#### 4. Discussion

Incorporation of Pb into natural ivanyukite-*Na-T* by the substitution scheme  $2\text{Na}^+ + 2\text{O}^{2-} \leftrightarrow \text{Pb}^{2+} + \square + 2\text{OH}^-$  results in its transformation into the cubic Pb-exchanged form. The same transition with increasing symmetry from  $R3m$  to  $P-43m$  was observed for the synthetic material and confirmed by powder X-ray diffraction (Figure 3) and Raman spectroscopy (Figure 2). During the Pb sorption, the significant decrease of the (101) reflection intensity and the appearance of additional peak at  $68.18^\circ 2\theta$ , instead of two peaks at  $67.15$  and  $68.80^\circ 2\theta$ , was observed. In the Raman spectra the shift for the most intense band at  $580\text{--}600\text{ cm}^{-1}$  to  $500\text{--}540\text{ cm}^{-1}$  related to the asymmetric bending vibrations of Si–O bonds or overlapping stretching vibrations of Ti–O bonds was observed. Such a shift was previously described for similar transitions in the ivanyukite-group minerals [27].

According to our chemical and sorption data, the maximal sorption capacity in relation to Pb was demonstrated by synthetic ivanyukite and reaches 400 mg/g at ambient conditions with synthetic ivanyukite. The maximal Pb content reaches 1.71 apfu. In the crystals structure of Pb-exchanged ivanyukite, the Pb1 site is situated at the center of the 8-MR and participates in the  $\text{OPb}_3$  triangles with the O–Pb distance of 2.954 Å (Figure 4b). Oxocentred triangles  $\text{OA}_3$  ( $A = \text{metal}$ ) are typical structural units in bismuth oxysalts with additional oxygen atoms [31,32], and was observed in Pb oxysalts as well [33].

There is a certain balance between the amounts of Pb in precipitates and the remaining solution. At the same time, there is an observed dependence of these amount from the NaCl content that is usually introduced at the beginning of the dust leaching process. When  $\text{Na}^+$  concentration is up to 200 g/L, the precipitation of Pb is seemingly incomplete. When the

$\text{Na}^+$  concentration is more than 200 g/L, no additional precipitation of trace amounts of Pb was observed.

In the case of the studied solutions, strongly acidic medium ( $\text{pH} < 1$ ) the fast protonation reactions in SIV and AM-4 titanosilicates is favored. In this case,  $\text{Na}^+$  cations should be quickly leaching into solution and two concurrent processes are observed described by the equations  $2\text{Na}^+ + \text{O}^{2-} \leftrightarrow 2\text{H}^+ + \text{OH}^-$  (protonation) and  $2\text{Na}^+ \leftrightarrow \text{Pb}^{2+}$  (ion-exchange).

It is known that  $\text{Pb}^{2+}$  cations in acidic chloride-sulfate solutions of metallurgical industries can form stable anionic complexes—such as  $[\text{PbCl}_3]^-$ ,  $[\text{PbCl}_4]^{2-}$ ,  $[\text{PbCl}_6]^{4-}$ , among others—which can be extracted from a solution on anion exchangers (e.g., AMP or AM-2b) with  $-\text{CH}_2\text{N}^+$ ,  $-\text{CH}_2\text{N}(\text{CH}_3)_2$ , and  $-\text{CH}_2\text{N}(\text{CH}_3)_3$  serving the role of exchange groups [34,35]. The sorption of Pb from acid mine drainage also includes its association to organic hydroxyl and carboxyl,  $\text{SiO}_4^{2-}$ , and  $-\text{R}-\text{O}-\text{H}$  functional groups [36,37]. The presence of carboxyl groups in some clay minerals also improves the adsorption of Pb [38]. In the case of titanosilicates used in this work, the key-role is presumably played by extra-framework sodium cations, which displacement may significantly affect the change in the surface charge of the samples. The SL3 material in this case is a good example of the formation of an intermediate between the product and the initial AM-4 phase leading to the change in the nature of the active centers of the material (decrease in the acidic strength of the active centers as a result of protonation) [19]. Since SL3 did not prove to be a good sorbent for Pb in our studies, we can assume that titanosilicate samples containing  $\text{Na}^+$  are required to decrease the stability of lead chloride complexes. In solutions with the content of  $\text{Cl}^-$  (20 g/L), extraction is observed with a high background of sodium in the solution (150 g/L) only. For this reason, it is important to determine and fix the mechanisms of the reactions taking place in natural ivanyukite crystals.

## 5. Conclusions

Occurrence of extra framework  $\text{Na}^+$  cations in the structure of titanosilicate sorbents plays a key role in Pb sorption. Both AM-4,  $\text{Na}_2\text{Ti}_2[\text{Si}_4\text{O}_{13}(\text{OH})] \cdot 2\text{H}_2\text{O}$  and SIV,  $\text{Na}_3\text{Ti}_4(\text{SiO}_4)_3\text{O}_4 \cdot 4\text{H}_2\text{O}$  titanosilicates with extra framework  $\text{Na}^+$  cations demonstrate 90% to 99% of Pb extraction from different solutions. At the same time SL3,  $\text{Ti}_2[\text{Si}_4\text{O}_{10}(\text{OH})_4]$ —protonated modification of AM-4 does not demonstrate good sorption properties. The maximal sorption capacity with respect to Pb is demonstrated by SIV and reaches 400 mg/g at ambient conditions. Both AM-4 and SIV may be recommended for the Pb sorption from the Pb-bearing dust leaching solution.

In solutions with the content of  $\text{Cl}^-$  (20 g/L), extraction was observed only with the high background of Na (150 g/L). It seems that  $\text{Na}^+$  ions neutralize  $\text{Cl}^-$ , which catalyzes the exchange reaction.

The molecular mechanism of incorporation of  $\text{Pb}^{2+}$  into ivanyukite structure by the substitution scheme  $2\text{Na}^+ + 2\text{O}^{2-} \leftrightarrow \text{Pb}^{2+} + \square + 2\text{OH}^-$  result in the structure transition with increasing symmetry from  $R\bar{3}m$  to  $P-43m$ . The symmetry transition has been confirmed by the SC XRD, PXRD, and Raman data. In the crystal structure of Pb-substituted form,  $\text{Pb}^{2+}$  cations occupy the centers of the 8-MRs and forms oxo-centered  $\text{OPb}_3$  units.

## 6. Patents

Nikolaev, A.I.; Samburov, G.O.; Kalashnikova, G.O.; Kasikov, A.G.; Panikorovskii, T.L.; Bazai, A.V. Method of silver extraction from pyrometallurgical wastes. Patent application RU 2021124566A, 16 February 2022.

**Supplementary Materials:** The following are available online at <https://www.mdpi.com/article/10.3390/cryst12030311/s1>, Table S1: Fractional Atomic Coordinates ( $\times 10^4$ ) and Equivalent Isotropic Displacement Parameters ( $\text{\AA}^2 \times 10^3$ ) for Pb-exchanged ivanyukite.  $U_{\text{eq}}$  is defined as 1/3 of the trace of the orthogonalised  $U_{\text{ij}}$  tensor; Table S2: Anisotropic Displacement Parameters ( $\text{\AA}^2 \times 10^3$ ) for Pb-exchanged ivanyukite. The Anisotropic displacement factor exponent takes the form:  $-2\pi^2[h^2a^2 \times U_{11} + 2hka \times b \times U_{12} + \dots]$ ; Table S3: Bond Lengths for Pb-exchanged ivanyukite.

**Author Contributions:** Conceptualization, V.N.Y. and A.K.; Methodology, G.O.S., G.O.K., A.V.B., E.S. and D.B.; Software, T.L.P. and V.N.B.; Validation, G.O.S., G.O.K., T.L.P., E.S., A.V.B., D.B. and A.K.; Formal analysis, E.S., D.B., T.L.P. and V.N.B.; Investigation, G.O.S., G.O.K., T.L.P. and E.S.; Resources, A.K. and V.N.Y.; Data curation, A.K. and S.V.K.; Writing—original draft preparation, G.O.S., T.L.P., G.O.K. and S.V.K.; Writing—review and editing, A.K., E.S., A.V.B., D.B. and S.V.K.; Visualization, T.L.P. and A.V.B.; Supervision, V.N.Y. and S.V.K.; Project administration, A.K.; Funding acquisition, G.O.S. and G.O.K. All authors have read and agreed to the published version of the manuscript.

**Funding:** This research was funded by the Ministry of Education and Science of the Murmansk Region, grant no. 244 at 2 September 2021 (synthesis of titanosilicates), by the Russian Foundation for Basic Research grant no. 20-33-90326 (sorption experiments) and Russian Science Foundation, project No. 21-77-10103 (SCXRD study).

**Institutional Review Board Statement:** Not applicable.

**Informed Consent Statement:** Not applicable.

**Data Availability Statement:** The CIF file contains data about the ivanyukite-Pb structure, Fractional Atomic Coordinates ( $\times 10^4$ ) and Equivalent Isotropic Displacement Parameters ( $\text{\AA}^2 \times 10^3$ ) for Pb-exchanged ivanyukite.  $U_{eq}$  is defined as 1/3 of the trace of the orthogonalised  $U_{ij}$  tensor, Anisotropic Displacement Parameters ( $\text{\AA}^2 \times 10^3$ ) for Pb-exchanged ivanyukite. The Anisotropic displacement factor exponent takes the form:  $-2\pi^2[h^2a \times ^2U_{11} + 2hka \times b \times U_{12} + \dots]$  and Bond Lengths for Pb-exchanged ivanyukite can be found at the link: <https://doi.org/10.5281/zenodo.6232628> (accessed on 30 January 2022).

**Acknowledgments:** The team of authors would like to acknowledge our professors from I.V. Tananaev Institute of Chemistry and Technology of Rare Elements and Mineral Raw Materials of the KSC RAS and Saint-Petersburg University—Britvin S.N., Gerasimova L.G., and Korovin V.N.—for their useful consultations, comments, and valuable advice regarding questions of hydrothermal synthesis of titanosilicates and features of chloride ligands in the complexes of platinum metals. The authors are also grateful to the X-ray Diffraction Centre, Geo Environmental Centre “Geomodel” of Saint-Petersburg State University for their help in our experimental studies.

**Conflicts of Interest:** The authors declare no conflict of interest.

## References

1. Yakovenchuk, V.N.; Nikolaev, A.P.; Selivanova, E.A.; Pakhomovsky, Y.A.; Korchak, J.A.; Spiridonova, D.V.; Zalkind, O.A.; Krivovichev, S.V. Ivanyukite-Na-T, ivanyukite-Na-C, ivanyukite-K, and ivanyukite-Cu: New microporous titanosilicates from the Khibiny massif (Kola Peninsula, Russia) and crystal structure of ivanyukite-Na-T. *Am. Mineral.* **2009**, *94*, 1450–1458. [[CrossRef](#)]
2. Popa, K.; Pavel, C.C.; Bilba, N.; Cecal, A. Purification of waste waters containing  $60\text{Co}^{2+}$ ,  $115\text{mCd}^{2+}$  and  $203\text{Hg}^{2+}$  radioactive ions by ETS-4 titanosilicate. *J. Radioanal. Nucl. Chem.* **2006**, *269*, 155–160. [[CrossRef](#)]
3. Kalashnikova, G.O.; Zhitova, E.S.; Selivanova, E.A.; Pakhomovsky, Y.A.; Yakovenchuk, V.N.; Ivanyuk, G.Y.; Kasikov, A.G.; Drogobuzhskaya, S.V.; Elizarova, I.R.; Kiselev, Y.G.; et al. The new method for obtaining titanosilicate AM-4 and its decationated form: Crystal chemistry, properties and advanced areas of application. *Microporous Mesoporous Mater.* **2021**, *313*, 110787. [[CrossRef](#)]
4. Cruciani, G.; De Luca, P.; Nastro, A.; Pattison, P. Rietveld refinement of the zorite structure of ETS-4 molecular sieves. *Microporous Mesoporous Mater.* **1998**, *21*, 143–153. [[CrossRef](#)]
5. Anthony, R.G.; Dosch, R.G.; Gu, D.; Philip, C.V. Use of silicotitanates for removing cesium and strontium from defense waste. *Ind. Eng. Chem. Res.* **1994**, *33*, 2702–2705. [[CrossRef](#)]
6. Men’shikov, Y.P.; Sokolova, E.V.; Egorov-Tismenko, Y.K.; Khomyakov, A.P.; Polezhaeva, L.I. Sitenakite,  $\text{Na}_2\text{KTi}_4\text{Si}_2\text{O}_{13}(\text{OH})\cdot 4\text{H}_2\text{O}$ —A new mineral. *Zap. RMO* **1992**, *121*, 94–99. (In Russian)
7. Panikorovskii, T.L.; Kalashnikova, G.O.; Nikolaev, A.I.; Perovskiy, I.A.; Bazai, A.V.; Yakovenchuk, V.N.; Bocharov, V.N.; Kabanova, N.A.; Krivovichev, S.V. Ion-Exchange-Induced Transformation and Mechanism of Cooperative Crystal Chemical Adaptation in Sitenakite: Theoretical and Experimental Study. *Minerals* **2022**, *12*, 248. [[CrossRef](#)]
8. Chapman, D.M.; Roe, A.L. Synthesis, characterization and crystal chemistry of microporous titanium-silicate materials. *Zeolites* **1990**, *10*, 730–737. [[CrossRef](#)]
9. Dadachov, M.; Rocha, J.; Ferreira, A.; Lin, Z.; Anderson, M. Ab initio structure determination of layered sodium titanium silicate containing edge-sharing titanate chains (AM-4)  $\text{Na}_3(\text{Na,H})\text{Ti}_2\text{O}_2[\text{Si}_2\text{O}_6]_2\cdot 2\text{H}_2\text{O}$ . *Chem. Commun.* **1997**, *3*, 2371–2372. [[CrossRef](#)]
10. Britvin, S.N.; Gerasimova, L.G.; Ivanyuk, G.Y.; Kalashnikova, G.O.; Krzhizhanovskaya, M.G.; Krivovichev, S.V.; Mararitsa, V.F.; Nikolaev, A.I.; Oginova, O.A.; Panteleev, V.N.; et al. Application of titanium-containing sorbents for treating liquid radioactive waste with the subsequent conservation of radionuclides in Synroc-type titanate ceramics. *Theor. Found. Chem. Eng.* **2016**, *50*, 598–606. [[CrossRef](#)]

11. Gerasimova, L.; Nikolaev, A.; Maslova, M.; Shchukina, E.; Samburov, G.; Yakovenchuk, V.; Ivanyuk, G. Titanite Ores of the Khibiny Apatite-Nepheline-Deposits: Selective Mining, Processing and Application for Titanosilicate Synthesis. *Minerals* **2018**, *8*, 446. [[CrossRef](#)]
12. Gerasimova, L.G.; Nikolaev, A.I.; Shchukina, E.S.; Maslova, M.V. Hydrothermal synthesis of framed titanosilicates with a structure of ivanyukite mineral. *Доклады Академии наук* **2019**, *487*, 289–292. [[CrossRef](#)]
13. Barcan, V.; Sylina, A. The appraisal of snow sampling for environmental pollution valuation. *Water. Air. Soil Pollut.* **1996**, *89*, 49–65. [[CrossRef](#)]
14. Yakovlev, E.; Druzhinina, A.; Druzhinin, S.; Zykov, S.; Ivanchenko, N. Assessment of physical and chemical properties, health risk of trace metals and quality indices of surface waters of the rivers and lakes of the Kola Peninsula (Murmansk Region, North-West Russia). *Environ. Geochem. Health* **2021**, 1–30. [[CrossRef](#)]
15. Barcan, V.; Kovnatsky, E. Soil Surface Geochemical Anomaly Around the Copper-Nickel Metallurgical Smelter. *Water. Air. Soil Pollut.* **1998**, *103*, 197–218. [[CrossRef](#)]
16. Koptsik, G.N.; Koptsik, S.V.; Smirnova, I.E.; Sinichkina, M.A. Remediation of Technogenic Barren Soils in the Kola Subarctic: Current State and Long-Term Dynamics. *Eurasian Soil Sci.* **2021**, *54*, 619–630. [[CrossRef](#)]
17. Nikolaev, A.I.; Samburov, G.O.; Kalashnikova, G.O. Method for the Extraction of Silver from Pyrometallurgical Waste. RU Patent Application No. 2021124566A, 16 February 2022.
18. Merlino, S.; Pasero, M.; Khomyakov, A.P. The crystal structure of lintisite,  $\text{Na}_3\text{LiTi}_2[\text{Si}_2\text{O}_6]_2\text{O}_2 \cdot 2\text{H}_2\text{O}$ , a new titanosilicate from Lovozero (USSR). *Z. Krist.* **1990**, *193*, 137–148. [[CrossRef](#)]
19. Timofeeva, M.N.; Kalashnikova, G.O.; Shefer, K.I.; Mel'gunova, E.A.; Panchenko, V.N.; Nikolaev, A.I.; Gil, A. Effect of the acid activation on a layered titanosilicate AM-4: The fine-tuning of structural and physicochemical properties. *Appl. Clay Sci.* **2020**, *186*, 105445. [[CrossRef](#)]
20. Gerasimova, L.G.; Shchukina, E.S.; Maslova, M.V.; Gladkikh, S.N.; Garaeva, G.R.; Kolobkova, V.M. Synthesis of rutile titanium dioxide from Russian raw materials. *Polym. Sci. Ser. D* **2017**, *10*, 23–27. [[CrossRef](#)]
21. Sheldrick, G.M. Crystal structure refinement with SHELXL. *Acta Crystallogr. Sect. C Struct. Chem.* **2015**, *71*, 3–8. [[CrossRef](#)]
22. Momma, K.; Izumi, F. VESTA 3 for three-dimensional visualization of crystal, volumetric and morphology data. *J. Appl. Crystallogr.* **2011**, *44*, 1272–1276. [[CrossRef](#)]
23. Frost, R.L.; Klopogge, J.T. Raman spectroscopy of some complex arsenate minerals—implications for soil remediation. *Spectrochim. Acta Part A Mol. Biomol. Spectrosc.* **2003**, *59*, 2797–2804. [[CrossRef](#)]
24. Filippi, M. Oxidation of the arsenic-rich concentrate at the Přebuz abandoned mine (Erzgebirge Mts., CZ): Mineralogical evolution. *Sci. Total Environ.* **2004**, *322*, 271–282. [[CrossRef](#)]
25. Filippi, M.; Doušová, B.; Machovič, V. Mineralogical speciation of arsenic in soils above the Mokrsko-west gold deposit, Czech Republic. *Geoderma* **2007**, *139*, 154–170. [[CrossRef](#)]
26. Yakovenchuk, V.; Pakhomovsky, Y.; Panikorovskii, T.; Zolotarev, A.; Mikhailova, J.; Bocharov, V.; Krivovichev, S.; Ivanyuk, G. Chirvinskyite,  $(\text{Na,Ca})_{13}(\text{Fe,Mn},\square)_2(\text{Ti,Nb})_2(\text{Zr,Ti})_3(\text{Si}_2\text{O}_7)_4(\text{OH,O,F})_{12}$ , a New Mineral with a Modular Wallpaper Structure, from the Khibiny Alkaline Massif (Kola Peninsula, Russia). *Minerals* **2019**, *9*, 219. [[CrossRef](#)]
27. Pakhomovsky, Y.A.; Panikorovskii, T.L.; Yakovenchuk, V.N.; Ivanyuk, G.Y.; Mikhailova, J.A.; Krivovichev, S.V.; Bocharov, V.N.; Kalashnikov, A.O. Selivanovaite,  $\text{NaTi}_3(\text{Ti,Na,Fe,Mn})_4(\text{Si}_2\text{O}_7)_2\text{O}_4(\text{OH,H}_2\text{O})_4 \cdot n\text{H}_2\text{O}$ , a new rock-forming mineral from the eudialyte-rich malnigne of the Lovozero alkaline massif (Kola Peninsula, Russia). *Eur. J. Mineral.* **2018**, *30*, 525–535. [[CrossRef](#)]
28. Krivovichev, S. Topology of Microporous Structures. *Rev. Mineral. Geochem.* **2005**, *57*, 17–68. [[CrossRef](#)]
29. Panikorovskii, T.L.; Yakovenchuk, V.N.; Yanicheva, N.Y.; Pakhomovsky, Y.A.; Shilovskikh, V.V.; Bocharov, V.N.; Krivovichev, S.V. Crystal chemistry of ivanyukite-group minerals,  $\text{A}_3 - x \text{H}_{1+x} [\text{Ti}_4\text{O}_4 (\text{SiO}_4)_3] (\text{H}_2\text{O})_n$  (A = Na, K, Cu), (n = 6–9, x = 0–2): Crystal structures, ion-exchange, chemical evolution. *Mineral. Mag.* **2021**, *85*, 607–619. [[CrossRef](#)]
30. Oleksienko, O.; Wolkersdorfer, C.; Sillanpää, M. Titanosilicates in cation adsorption and cation exchange—A review. *Chem. Eng. J.* **2017**, *317*, 570–585. [[CrossRef](#)]
31. Rumsey, M.S.; Mills, S.J.; Spratt, J. Natropharmacoalumite,  $\text{NaAl}_4[(\text{OH})_4(\text{AsO}_4)_3] \cdot 4\text{H}_2\text{O}$ , a new mineral of the pharmacosiderite supergroup and the renaming of aluminopharmacosiderite to pharmacoalumite. *Mineral. Mag.* **2010**, *74*, 929–936. [[CrossRef](#)]
32. Bedlivy, D.; Mereiter, K. Preisingerite,  $\text{Bi}_3\text{O}(\text{OH})(\text{AsO}_4)_2$ , a new species from San Juan Province, Argentina: Its description and crystal structure. *Am. Mineral.* **1982**, *67*, 833–840.
33. Ridkosil, T.; Srein, V.; Fabry, J.; Hybler, J.; Maximov, B.A. Mrazekite,  $\text{Bi}_2\text{Cu}_3(\text{OH})_2\text{O}_2(\text{PO}_4)_2$ . *Can. Mineral.* **1992**, *30*, 215–224.
34. Siidra, O.I.; Zinyakhina, D.O.; Zadoya, A.I.; Krivovichev, S.V.; Turner, R.W. Synthesis and Modular Structural Architectures of Mineralogically Inspired Novel Complex Pb Oxyhalides. *Inorg. Chem.* **2013**, *52*, 12799–12805. [[CrossRef](#)]
35. Voropanova, L.A.; Gagieva, Z.A.; Pukhova, V.P.; Vil'ner, N.A. Method of Extracting Lead Ions  $\text{Pb}^{2+}$  from Acidic Solutions. RU Patent Application No. 2393244C1, 2010.
36. Lu, H.; Zhang, W.; Yang, Y.; Huang, X.; Wang, S.; Qiu, R. Relative distribution of  $\text{Pb}^{2+}$  sorption mechanisms by sludge-derived biochar. *Water Res.* **2012**, *46*, 854–862. [[CrossRef](#)]
37. Wang, Q.; Zheng, C.; Cui, W.; He, F.; Zhang, J.; Zhang, T.C.; He, C. Adsorption of  $\text{Pb}^{2+}$  and  $\text{Cu}^{2+}$  ions on the CS2-modified alkaline lignin. *Chem. Eng. J.* **2020**, *391*, 123581. [[CrossRef](#)]
38. Pavlovic, I.; Perez, M.; Barriga, C.; Ulibarri, M. Adsorption of  $\text{Cu}^{2+}$ ,  $\text{Cd}^{2+}$  and  $\text{Pb}^{2+}$  ions by layered double hydroxides intercalated with the chelating agents diethylenetriaminepentaacetate and meso-2,3-dimercaptosuccinate. *Appl. Clay Sci.* **2009**, *43*, 125–129. [[CrossRef](#)]